

Optical and Neutron Inelastic Scattering Study of 2-Methylnorbornanes

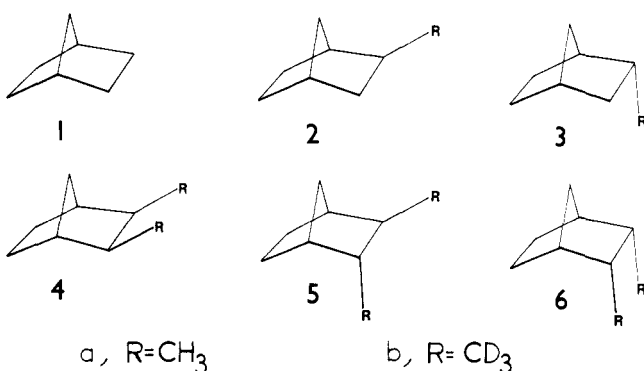
Yvon Brunel,[†] Christian Coulombeau,*[†] Christiane Coulombeau,[†] and Hervé Jobic[‡]

LEDSS VI, Domaine Universitaire, BP No. 68, 38402 Saint-Martin-d'Hères Cedex, France; L.A. 332, CNRS 15, and Institut Lauë Langevin, 156 X, 38402 Grenoble Cedex, France (Received: October 2, 1984)

We have measured the infrared, Raman, and neutron vibrational spectra of the 2-methylnorbornanes with a CH₃ or CD₃ methyl group in the exo or endo position. A normal coordinate analysis has been carried out. The torsional modes of the methyl group are assigned at 240 and 235 cm⁻¹ for the hydrogenated exo and endo isomers, respectively. The corresponding barrier is 15.2 ± 0.2 kJ mol⁻¹. The calculated neutron intensities are in good agreement with the experimental data. The frequencies are used for the determination of the thermodynamic contribution to the standard free energy difference.

Introduction

We have started a vibrational investigation of highly strained systems: the norbornane molecule (1) and some of its derivatives,



the 2-methylnorbornanes (2, and 3) and the 2,3-dimethylnorbornanes (4-6). For these molecules the steric interactions, which may induce vibrational frequency shifts, can be evaluated, after a force field calculation, from the principal and interaction force constants values as well as from the normal-coordinate atomic motions.

For this purpose it is necessary to determine all the experimental frequencies and to make a proper assignment which can be tested by a normal-coordinate analysis. Since the low-frequency vibrations have a predominant role in the entropy and heat capacity differences between isomers, we have concentrated our work on the low-frequency range of vibration.

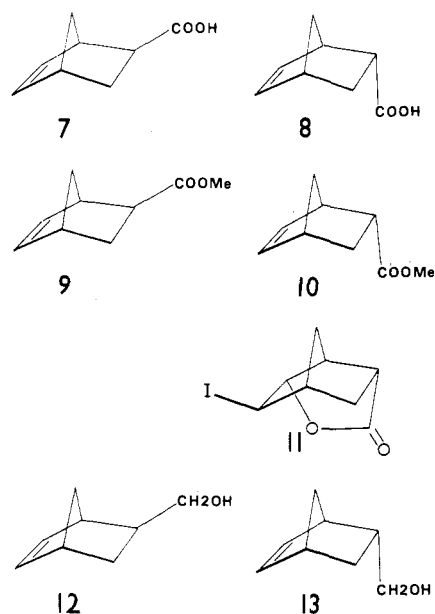
In our first paper, we reanalyzed the vibrational data for the norbornane molecule (1) using optical and neutron spectroscopies.¹ Our second step is to assign the vibrational spectra of the monomethyl derivatives (2 and 3). It is already known from molecular mechanics calculations² and chemical equilibration³ that the exo isomer (2) is more stable than the endo isomer (3). This difference in stability was accounted for by the steric interactions between the methyl group and the skeletal framework.⁴

We report in this paper an optical and neutron spectroscopic study of the 2-methylnorbornanes (2 and 3). We have measured the infrared and Raman spectra of totally hydrogenated molecules (2a and 3a) and of selectively deuterated compounds (2b and 3b). In the low-frequency range (10-500 cm⁻¹), we have used neutron inelastic spectroscopy (NIS) to observe the transitions which are weak or inactive in the infrared or Raman, e.g., the methyl torsional modes.

Experimental Section

Preparation. We have synthesized *exo*- and *endo*-2-methylbicyclo[2.2.1]heptane (2a and 3a) and *exo*- and *endo*-2-(tri-deuteriomethyl)bicyclo[2.2.1]heptane (2b and 3b) from a mixture

of the two bicyclo[2.2.1]hept-5-ene-2-carboxylic acids 7 and 8.



Preparation of the Carboxylic Acids 7 and 8 Mixture. The mixture can be obtained (1) from a Diels-Alder condensation of cyclopentadiene with acrylic acid at 0 °C (the ratio of *exo* 7 to *endo* 8 adducts is 1:3⁵) and (2) from a Diels-Alder addition of methyl acrylate to cyclopentadiene followed by saponification of the adducts 9 and 10. The ratio of the isomeric esters 9 and 10 is influenced by solvents, temperature, and catalysts.⁶⁻⁹ The saponification of various mixtures of 9 and 10 in refluxing methanolic potassium hydroxide or in refluxing diethylene glycol-potassium hydroxide solutions produces the two acids (7 and 8) in an isomeric ratio of 1:1. A better ratio of *exo* acid 7 cannot be obtained.

Preparation of Pure Bicyclo[2.2.1]hept-5-ene-2-endo-carboxylic Acid (8). Iodolactonization of the mixture^{7,10} of acids 7 and 8 (isomeric ratio 1:3 or 1:1) leads to iodolactone 11 and unchanged *exo* acid 7 due to the unsuitable configuration for lactonization.

Extraction of iodolactone in a basic medium followed by two crystallizations from ethyl acetate/*n*-hexane gives pure iodolactone

(1) Brunel, Y.; Coulombeau, C.; Coulombeau, C.; Moutin, M.; Jobic, H. *J. Am. Chem. Soc.* **1983**, *105*, 6411.

(2) Brunel, Y.; Coulombeau, C.; Rassat, A. *Nouv. J. Chim.* **1980**, *4*, 663.

(3) Ouellette, R. J.; Rawn, J. D.; Jreissaty, S. N. *J. Am. Chem. Soc.* **1971**, *93*, 7117.

(4) Altona, C.; Sundaralingam, M. *J. Am. Chem. Soc.* **1970**, *92*, 1995.

(5) Le Drian, C., Thèse d'Etat, Grenoble, 1981.

(6) Parlar, H.; Baumann, R. *Angew. Chem., Int. Ed. Engl.* **1981**, *20*, 1014.

(7) Sauer, J.; Kredel, J. *Tetrahedron Lett.* **1966**, *51*, 6359.

(8) Sauer, J.; Kredel, J. *Angew. Chem., Int. Ed. Engl.* **1966**, *4*, 989.

(9) Alder, K.; Stein, G. *Annalen* **1934**, *514*, 197.

(10) Ver Nooy, C. D.; Røndestvedt, C. S., Jr. *J. Am. Chem. Soc.* **1955**, *77*, 3583.

[†]LEDSS VI.

[‡]Institut Lauë Langevin. Present address: Institut de Recherches sur la Catalyse, 2, Avenue Albert Einstein, 69626 Villeurbanne Cedex, France.

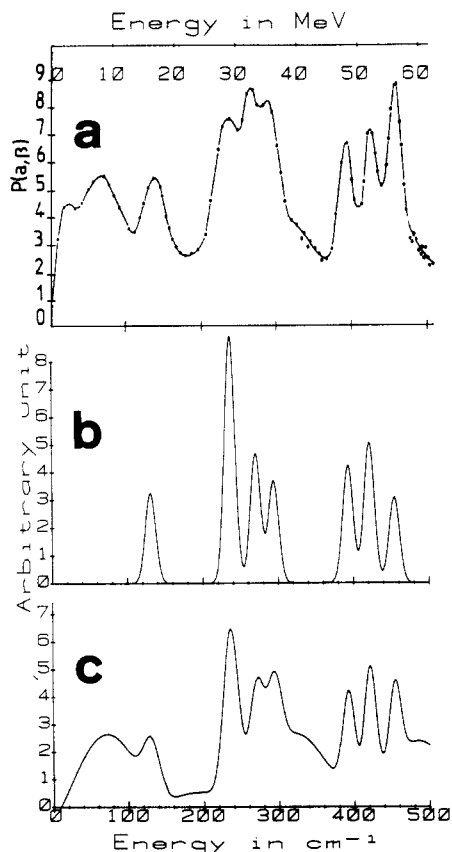
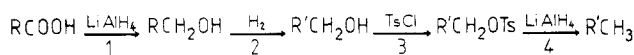


Figure 1. NIS spectra of *exo*-2-methylnorbornane (**2a**): (a) experimental spectrum obtained on IN4; (b) spectrum simulated with a constant resolution; (c) simulated spectrum including the combination modes and the instrumental resolution.

(11). The iodolactone treated with zinc in acetic acid leads to pure *endo* acid **8**.⁷

Preparation of 2-exo-Hydroxymethylbicyclo[2.2.1]hept-5-ene (12). Unreacted *exo* acid **7** recovered after iodolactonization is not very pure; small amounts of *endo* acid **8** remain and attempts to purify it by crystallization failed. A reduction of the acid mixture with lithium aluminum hydride followed by chromatography either on an alumina column or in the gaseous phase resulted in the recovery of pure *exo* alcohol **12**. Chromatography is only useful with the mixture composed almost exclusively of *exo* alcohol **12**; it failed with the alcohol **12**-**13** mixture in an isomeric ratio of 1:1.

Preparation of 2-Methyl- and 2-(Trideuteriomethyl)bicyclo[2.2.1]heptane (2a, 3a, 2b, and 3b). The reactions leading to the synthesis of **2a** and **3a** from acids **7** and **8** are as follows:



The deuterated derivatives **2b** and **3b** are synthesized via the same sequence using lithium aluminum deuteride instead of lithium aluminum hydride in steps 1 and 4. Finally, compounds **2a**, **3a**, **2b**, and **3b** are purified by passage through a column filled with alumina containing 18% silver nitrate to remove the toluene formed in step 4. The chemical purity was determined by gas-chromatography and by ¹³C nuclear magnetic resonance¹¹ (it was found to be >97%). The overall yield for the two steps described in the above scheme is 45%. A mixture of **2b** and **3b** in an isomeric

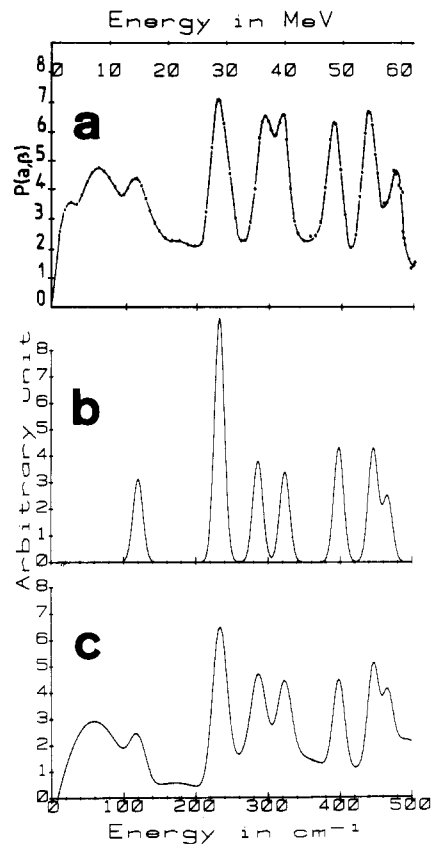


Figure 2. NIS spectra of *endo*-2-methylnorbornane (**3a**): (a) experimental spectrum obtained on IN4; (b) spectrum simulated with a constant resolution; (c) simulated spectrum including the combination modes and the instrumental resolution.

ratio of 1:3 used for the first NIS experiment was obtained from a Diels-Alder condensation of cyclopentadiene with acrylic acid at 0 °C followed by the reactions in the scheme above.

Vibrational Spectra. The experimental conditions were the same as for norbornane.¹ The infrared and Raman spectra were obtained with the pure liquids at room temperature. The vibrational frequencies were also studied by NIS at the Institut Laue Langevin (I.L.L.); the frequency range 10–500 cm⁻¹ was recorded on a IN4 time-of-flight spectrometer and the region 200–1600 cm⁻¹ on the beryllium filter detector IN1 spectrometer.

However, at the time of the neutron experiment on IN4, we had only pure compounds **2a** and **3a** and a mixture of **2b** (72 ± 2%) and **3b** (28 ± 2%) (the relative proportions were determined from ¹³C NMR spectroscopy). The 3 NIS spectra obtained on IN4 at 6 K are shown in the upper part of Figures 1–3. All pure compounds were reinvestigated on IN1 at 10 K; the spectra of compounds **2b** and **3b** are shown in Figures 4a and 5a, respectively.

Because the accuracy on the frequency values is better in optical spectroscopy than in neutron spectroscopy, we have used the Raman optical data in the refinement process. The frequency values are given in Tables I and II.

Normal-Coordinate Calculations

The frequencies and mass-weighted eigenvectors were obtained by the standard GF matrix method.¹²

Geometry. For the G matrix calculation, no structural parameters are available for the 2-methylnorbornanes. For the norbornane molecule itself, precise carbon-carbon bond lengths are difficult to obtain, even when electron diffraction is combined with spectroscopic data and ab-initio calculations.¹³ Therefore it is doubtful that this method could be applied to the 2-

(12) Wilson, E. B.; Decius, J. C.; Cross, P. C. "Molecular Vibrations"; McGraw-Hill: New York, 1955.

(13) Doms, L.; Van den Enden, L.; Geise, H. J.; Van Alsenoy, C. *J. Am. Chem. Soc.* **1983**, *105*, 158.

(11) Grutzner, J. B.; Jautelat, M.; Dence, J. B.; Smith, R. A.; Roberts, J. D. *J. Am. Chem. Soc.* **1970**, *92*, 7107.

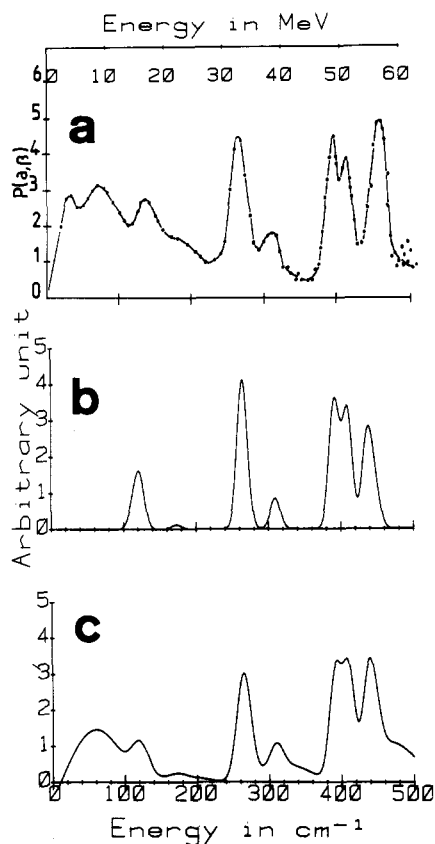


Figure 3. NIS spectra of 2-(trideuteriomethyl)norbornane **2b** + **3b** mixture: (a) experimental spectrum obtained on IN4; (b) spectrum simulated with a constant resolution; (c) simulated spectrum including the combination modes and the instrumental resolution.

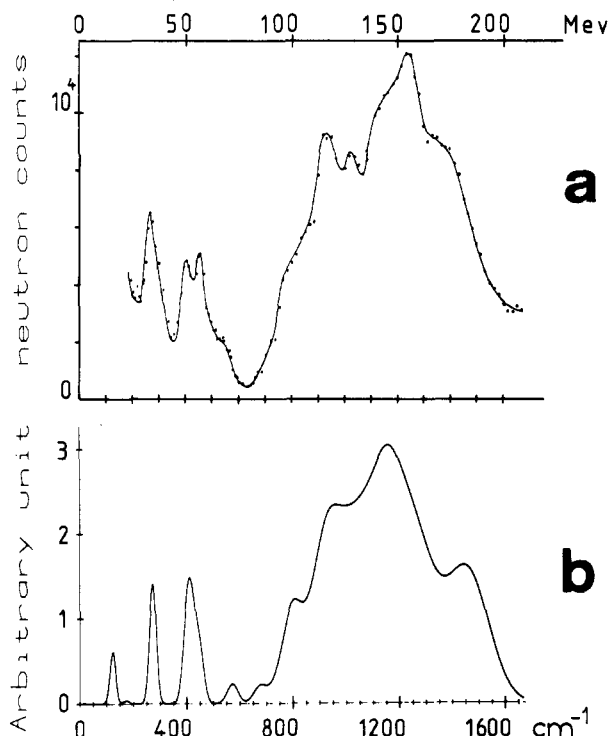


Figure 4. NIS spectra of *exo*-2-(trideuteriomethyl)norbornane **2b**: (a) experimental spectrum obtained on IN1; (b) spectrum simulated with the instrumental resolution.

methylnorbornanes. An X-ray structure determination would also be difficult because the 2-methylnorbornanes are liquid at room temperature. Furthermore, we have found by differential scanning calorimetry that these compounds exhibit two distinct plastic phases, as do the parent norbornane molecule.¹⁴ Since no de-

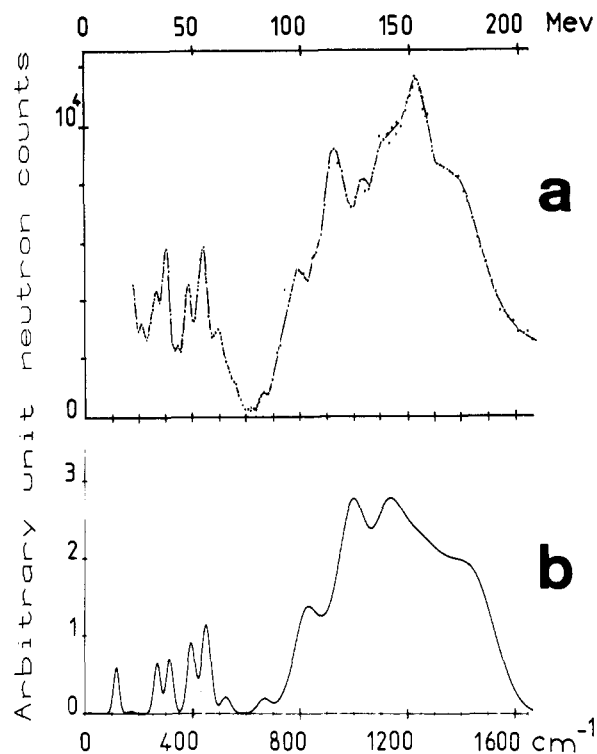


Figure 5. NIS spectra of *endo*-2-(trideuteriomethyl)norbornane (**3b**): (a) experimental spectrum obtained on IN1; (b) spectrum simulated with the instrumental resolution.

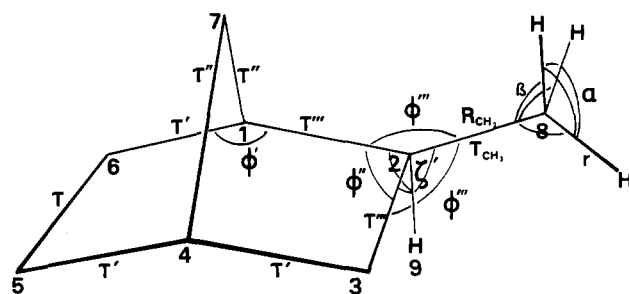


Figure 6. Internal coordinates used in the 2-methylnorbornanes: for the bicyclic system, the internal coordinates are those of norbornane;¹ the internal coordinates of the methyl groups, bonds, valence angles, or dihedral angles defined several times are indicated.

formation of the skeletal framework can be justified a priori, we have kept the same geometry for the norbornane moiety.¹⁵ We have added the methyl group, in a staggered configuration, with standard bond lengths and valence angles ($CC = 1.540 \text{ \AA}$; $CH = 1.115 \text{ \AA}$, and $CCH = 109.5^\circ$). We think that this approximation is reasonable since the calculated frequencies are more sensitive to variations in the force constants than in the bond length values.

Force Field. The initial force field for the norbornane moiety was obtained in our previous work.¹ For the methyl group we have taken the force constants from the work of Snyder and Schachtschneider.¹⁶ The interactions between the two moieties are taken into account by differentiating the force constants corresponding to the angles $C_1C_2C_3$ ($H_{\phi''}$), $C_1C_2C_8$ ($H_{\phi'''}$), and $C_1C_2H_9$ ($H_{\tau'}$) and the interaction constants $F_{\phi''\phi'''}$ and $f_{\phi''\phi'''}$ (see Figure 6).

The least-squares refinement was performed simultaneously on the frequencies of one isomer and its deuterated derivative:

(14) Jackson, R. L.; Strange, J. H. *Acta Crystallogr., Sect. B* **1972**, *28*, 1645.

(15) (a) Yokozeki, A.; Kuchitsu, K. *Bull. Chem. Soc. Jpn.* **1971**, *44*, 2356. (b) Chiang, J. F.; Wilcox, C. F., Jr.; Bauer, S. H. *J. Am. Chem. Soc.* **1968**, *90*, 3149.

(16) Snyder, R. G.; Schachtschneider, J. H. *Spectrochim. Acta* **1965**, *21*, 169.

TABLE I: Observed and Calculated Vibration Modes for the 2-*exo*-Methylnorbornanes 2a and 2b along with Their Potential Energy Distribution (PED)^a

no.	NIS	IR	Raman	calcd	PED	NIS	IR	Raman	calcd	PED
15		1476	1484	1484	$H_\beta(78); H_\gamma(25)$	1476	1485	1484	$H_\beta(78); H_\gamma(25)$	
16		1450	1454	1459	$H_\beta(81); H_\gamma(22)$		1455	1459	$H_\beta(81); H_\gamma(22)$	
17			1453	1454	$H_\beta(81); H_\gamma(21)$		1453	1454	$H_\beta(81); H_\gamma(21)$	
18			1459	1447	$H_\beta(83); H_\gamma(20)$	1445	1452	1447	$H_\beta(83); H_\gamma(20)$	
19		1450	1440	1439	$H_\alpha(85); H_\beta(10)$		1360	1372	$K_R(29); K_{R(Me)}(17); H_\gamma(17); H_\gamma(11)$	
20			1440	1435	$H_\alpha(91)$	1338	1344	1325	$K_R(13); K_R(40); H_\gamma(33)$	
21		1373	1379	1376	$K_R(24); K_{R(Me)}(24); H_\gamma(14); H_\gamma(16)$	1312	1328	1321	$K_R(11); K_R(47); H_\gamma(32); H_\gamma(10)$	
22		1346	1351	1354	$H_\alpha(41); H_\beta(49)$	1302	1307	1312	$K_R(48); H_\gamma(36); H_\beta(13)$	
23		1313	1318	1327	$K_R(14); K_R(37); H_\gamma(30)$	1284	1288	1286	$K_R(22); K_R(17); H_\gamma(33); K_\gamma(14)$	
24			1318	1321	$K_R(47); H_\gamma(32)$	1272	1278	1275	$K_R(34); H_\gamma(59)$	
25		1303	1310	1312	$K_R(47); H_\gamma(38); H_\beta(13)$	1256	1265	1269	$K_R(19); H_\gamma(37); H_\gamma(16); H_\gamma(19)$	
26		1286	1290	1287	$K_R(19); K_R(18); H_\gamma(29); H_\gamma(27)$	1242	1248	1250	$H_\gamma(61); H_\gamma(23)$	
27		1274	1280	1277	$K_R(34); H_\gamma(57)$		1222	1224	$H_\gamma(47); H_\gamma(18); H_\gamma(19)$	
28		1262	1268	1269	$K_R(19); H_\gamma(41); H_\gamma(19); H_\gamma(15)$	1216	1215	1210	$K_R(11); H_\gamma(44); H_\gamma(26)$	
29		1246	1251	1250	$H_\gamma(62); H_\gamma(23)$	1170	1176	1183	$H_\gamma(64)$	
30		1222	1228	1230	$H_\alpha(36); H_\gamma(22); H_\gamma(17)$	1152	1154	1150	$K_R(17); H_\gamma(39); H_\gamma(25)$	
31		1212	1212	1213	$H_\alpha(56); H_\gamma(20)$	1140	1145	1152	$H_\gamma(57); H_\gamma(15)$	
32		1178	1184	1183	$H_\gamma(67)$	1128	1133	1130	$K_{R(Me)}(10); H_\gamma(34); H_\gamma(16); H_\gamma(13)$	
33		1164	1169	1156	$K_R(11); H_\gamma(51); H_\gamma(18)$	1101	1120	1119	$K_{R(Me)}(14); H_\gamma(33); H_\gamma(22); H_\gamma(10)$	
34		1142	1148	1149	$K_R(16); H_\gamma(48); H_\gamma(24)$		1083	1078	$H_\gamma(18); H_\gamma(17); H_\gamma(29)$	
35		1114	1121	1126	$H_\alpha(46); H_\gamma(29)$	1055	1059	1054	$H_\gamma(38); H_\gamma(22)$	
36		1102	1107	1100	$H_\alpha(20); H_\gamma(14); H_\gamma(29)$	1038	1044	1047	$H_\gamma(46); H_\gamma(20)$	
37		1069	1075	1081	$H_\beta(23); H_\gamma(18); H_\gamma(13); H_\gamma(14)$		1026	1031	$H_\alpha(83)$	
38		1058	1050	1054	$H_\alpha(51); H_\gamma(24)$	1020	1026	1029	$H_\alpha(95)$	
39		1030	1037	1039	$H_\beta(30); H_\gamma(14)$	1006	1011	1001	$H_\gamma(39); H_\gamma(31)$	
40		1015	1020	1019	$H_\beta(33); H_\gamma(32); H_\gamma(14)$	986	993	982	$K_R(26); H_\gamma(27); H_\gamma(12)$	
41		990	996	1001	$H_\alpha(34); H_\gamma(32)$	950	956	962	$K_R(20); H_\gamma(56)$	
42		968	973	987	$K_R(12); H_\beta(15); H_\gamma(29); H_\gamma(12)$		934	929	$K_R(39); H_\gamma(18)$	
43			958	959	$K_R(35); H_\gamma(39)$	928	924	930	$K_R(13); K_R(31); H_\beta(14)$	
44		952	949	946	$K_R(30); H_\gamma(36)$	918	914	919	$K_R(18); H_\gamma(47)$	
45		920	926	928	$K_R(53); H_\gamma(17)$	886	892	907	$K_R(31); H_\gamma(30)$	
46		898	904	898	$H_\gamma(64)$	878	884	874	$K_R(29); K_R(23); H_\gamma(17)$	
47		871	873	875	$K_R(35); K_R(27); H_\gamma(17)$	856	862	846	$K_R(15); K_R(17); H_\beta(13); H_\gamma(28)$	
48		834	840	857	$K_R(12); K_R(47); H_\gamma(25)$	820	825	809	$H_\beta(30); H_\gamma(35)$	
49		812	817	825	$K_R(27); H_\gamma(40)$	794	782	791	$K_R(10); K_R(12); H_\gamma(36)$	
50		793	799	789	$K_R(19); K_R(18); H_\gamma(38)$	776	770	776	$K_R(40); H_\beta(13); H_\omega(14)$	
51		758	764	757	$K_R(31); K_R(13); H_\beta(12)$	734	737	735	$K_R(22); K_R(14); H_\beta(30)$	
52		720	727	714	$K_R(41); K_{R(Me)}(14); H_\omega(14)$	678	684	678	$K_R(33); K_{R(Me)}(14); H_\beta(15); H_\omega(14)$	
53		578	583	594	$H_\alpha(23); H_\alpha(34); H_{\phi''}(11)$	556	559	572	$H_\beta(14); H_\alpha(21); H_\alpha(32); H_{\phi''}(13)$	
54	469	468	471	464	$H_\alpha(33); H_{\phi''}(17)$	461	452	455	$H_\alpha(50); H_{\phi''}(10)$	
55	434	433	437	431	$H_\gamma(12); H_\alpha(35); H_{\phi''}(21); H_{\phi''}(27)$	417	412	415	$H_\gamma(12); H_\alpha(26); H_{\phi''}(30); H_\gamma(12)$	
56	401	398	402	403	$H_\gamma(16); H_\alpha(47); H_{\phi''}(53)$	396	394	396	$H_\gamma(14); H_\alpha(42); H_{\phi''}(53)$	
57	298	300	301	300	$H_\alpha(16); H_{\phi''}(13); H_{\phi''}(60)$	263	275	266	$268 H_\alpha(13); H_{\phi''}(22); H_{\phi''}(23); H_\gamma(38)$	
58	274	276	274	275	$H_\alpha(13); H_{\phi''}(24); H_{\phi''}(20); H_\gamma(35)$	263	264	266	$273 H_\gamma(11); H_\alpha(11); H_{\phi''}(64)$	
59	240		241		$H_{\gamma(Me)}(89)$	175		173	$H_{\gamma(Me)}(96)$	
60	135	137	131		$H_\alpha(20); H_\beta(10); H_{\phi''}(15); H_\gamma(29); H_{\phi''}(22)$	128	125	123	$H_\alpha(19); H_\alpha(11); H_{\phi''}(17); H_\gamma(27); H_{\phi''}(22)$	

^aThe average error is 5.0 cm⁻¹ or 0.60%.

(2a) + (2b) and (3a) + (3b). The final force field which includes 41 force constants for each isomer is shown in Table III.

Interpretation of Results

From the first normal-coordinate analysis using the initial force constants, seven frequencies were found below 500 cm⁻¹. This is in good agreement with the seven peaks observed on IN4, between 100 and 500 cm⁻¹, for each hydrogenated compound (Figures 1a and 2a).

Above 500 cm⁻¹, the NIS spectra obtained on IN1 yield only envelopes (Figures 4a and 5a). These spectra can be useful to test the assignment but the frequency values used for the refinement have to be taken from the optical spectra.

As for the norbornane molecule¹ the assignment of the high-frequency modes contains a few uncertainties: (i) the number of experimental peaks observed in IR, Raman, or NIS is lower than the number of expected frequencies (3N - 6 = 60) and (ii) the ν_{CH} stretching region shows only unresolved broad bands in the IR or Raman, making the assignment difficult.

The initial assignment was progressively modified during the refinement cycles. As in our previous work,¹ two criteria have been considered: the average error between the experimental and calculated frequencies and the comparison between the experimental and simulated NIS spectra.

Because of the increased number of vibrational modes in the IN4 range, we have improved the simulation of the NIS spectrum by including the resolution of the spectrometer and by considering the combinations of the fundamentals with the lattice modes. These combinations not only produce weak bands, e.g., at 330 cm⁻¹ for 2a and at 175 cm⁻¹ for 3a, but they also alter the NIS intensities of the fundamentals when they are too close in frequency to be resolved. Their contribution to the NIS profile has to be taken into account if one wants to obtain a good agreement between the experimental and calculated spectra.

The scattering law, for a process in which a neutron loses n_k quanta of energy $\hbar\omega_k$, is defined by¹⁷

$$S_n(Q, \omega) = \sum_d \prod_k \left[\exp(-2W_d) \frac{1}{(n_k)!} \left(\frac{\hbar(Q \cdot C_d^k)^2}{2m\omega_k} \right)^{n_k} \delta(\omega - \sum_k n_k \omega_k) \right]$$

This expression is valid for hydrogenated samples at low temperatures; $\hbar Q$ is the neutron momentum transfer, m the hydrogen atom mass, and C_d^k the displacement vector for the d th proton in the k th normal mode. It has been recently shown that the

TABLE II: Observed and Calculated Vibration Modes for the 2-endo-Methylnorbornanes 3a and 3b along with Their PED^a

no.	NIS	IR	Raman	calcd	PED	NIS	IR	Raman	calcd	PED
15		1480	1483	1486	$H_\beta(73); H_\gamma(27)$		1478	1478	1486	$H_\beta(73); H_\gamma(27)$
16		1451	1453	1457	$H_\alpha(77)$		1453	1453	1451	$H_\beta(76); H_\gamma(25)$
17			1453	1451	$H_\beta(74); H_\gamma(24)$			1453	1448	$H_\beta(75); H_\gamma(24)$
18			1453	1455	$H_\alpha(91)$			1453	1442	$H_\beta(74); H_\gamma(25)$
19			1440	1447	$H_\beta(68); H_\gamma(21)$			1380	1370	$K_R(\text{Me})(10); H_\gamma(83)$
20			1440	1442	$H_\beta(74); H_\gamma(25)$		1339	1342	1357	$K_R(19); H_\gamma(13); H_\gamma(67)$
21	1374		1378	1385	$H_\alpha(35); H_\beta(41); H_\gamma(18)$		1322	1325	1321	$K_R(47); H_\gamma(43); H_\gamma(25)$
22			1378	1366	$H_\alpha(12); H_\beta(15); H_\gamma(65)$		1308	1311	1314	$K_R(27); H_\gamma(33); H_\gamma(47)$
23	1344		1348	1357	$K_R(19); H_\gamma(13); H_\gamma(65)$		1300	1302	1300	$K_R(14); K_R(27); H_\gamma(50); H_\gamma(16)$
24	1320		1327	1322	$K_R(46); H_\gamma(41); H_\gamma(26)$		1275	1279	1284	$K_R(11); H_\gamma(45); H_\gamma(41)$
25			1310	1314	$K_R(27); H_\gamma(34); H_\gamma(45)$		1257	1261	1258	$K_R(53); H_\gamma(53)$
26	1300		1302	1300	$K_R(14); K_R(27); H_\gamma(50); H_\gamma(16)$		1246	1245	1241	$K_R(29); K_R(27); H_\gamma(51); H_\gamma(16)$
27	1276		1282	1283	$K_R(11); H_\gamma(45); H_\gamma(40)$		1234	1240	1234	$K_R(27); H_\gamma(43); H_\gamma(37)$
28	1257		1259	1258	$K_R(52); H_\gamma(53)$		1210	1213	1219	$H_\gamma(75)$
29	1247		1238	1241	$K_R(30); K_R(27); H_\gamma(51); H_\gamma(16)$		1173	1175	1188	$K_R(16); H_\gamma(37); H_\gamma(27)$
30	1235		1233	1234	$K_R(27); H_\gamma(43); H_\gamma(37)$		1164	1170	1164	$K_R(22); H_\gamma(23); H_\gamma(46)$
31	1214		1219	1219	$H_\gamma(76)$		1134	1136	1134	$H_\gamma(74); H_\gamma(21)$
32	1178		1182	1186	$K_R(16); H_\gamma(41); H_\gamma(31)$			1136	1127	$K_R(\text{Me})(21); H_\alpha(16); H_\beta(19); H_\gamma(32)$
33	1166		1173	1164	$K_R(24); H_\gamma(27); H_\gamma(42)$		1114	1116	1117	$H_\gamma(56); H_\gamma(16)$
34			1130	1134	$H_\gamma(73); H_\gamma(22)$		1076	1080	1098	$H_\gamma(47); H_\gamma(25)$
35	1128		1130	1121	$H_\gamma(68); H_\gamma(20)$		1066	1068	1072	$K_R(10); H_\gamma(53); H_\gamma(18)$
36	1107		1114	1104	$H_\gamma(46); H_\gamma(24)$		1048	1052	1047	$H_\alpha(88)$
37	1078		1081	1081	$K_R(15); H_\beta(12); H_\gamma(37); H_\gamma(16)$			1052	1046	$H_\alpha(92)$
38	1058		1062	1043	$H_\gamma(41); H_\beta(19)$			1009	1003	$K_R(13); K_R(13); H_\gamma(49); H_\gamma(11)$
39			1030	1030	$K_R(\text{Me})(19); H_\beta(14); H_\gamma(29); H_\gamma(13)$		1008	1009	1015	$K_R(10); H_\gamma(55)$
40	1016		1018	1023	$H_\beta(21); H_\gamma(54)$			998	1000	$K_R(20); H_\gamma(50)$
41	987		991	997	$K_R(21); H_\gamma(50); H_\gamma(12)$		993	998	991	$K_R(25); H_\gamma(44)$
42	966		970	977	$K_R(25); K_R(\text{Me})(10); H_\beta(15); H_\gamma(31); H_\gamma(10)$		953	960	963	$K_R(51); H_\gamma(23)$
43			960	966	$K_R(42); H_\gamma(34)$		940	944	946	$K_R(61); H_\gamma(33)$
44	946		951	959	$K_R(16); H_\beta(31); H_\gamma(30)$		923	926	926	$K_R(21); K_R(26); H_\gamma(11)$
45	928		930	948	$K_R(46); H_\gamma(22)$		879	883	884	$K_R(52); H_\gamma(28)$
46	920		924	926	$K_R(44); H_\beta(21); H_\gamma(17)$		853	854	858	$K_R(45); K_R(31); H_\gamma(20)$
47	898		900	878	$K_R(50); H_\gamma(30)$		822	827	829	$H_\beta(16); H_\gamma(56)$
48	872		875	859	$K_R(44); K_R(33); H_\gamma(20)$		802	804	806	$H_\beta(34); H_\gamma(36)$
49	822		825	820	$H_\gamma(77)$		779	778	789	$K_R(17); H_\beta(24); H_\beta(15)$
			803		482 + 322					
50	790		798	790	$K_R(40); K_R(23); K_R(\text{Me})(18)$		768	770	764	$K_R(11); K_R(28); H_\beta(12)$
51	756		758	764	$K_R(22); K_R(16); H_\beta(23); H_\omega(11)$		737	739	728	$K_R(21); H_\beta(55)$
52	716		719	713	$K_R(30); H_\gamma(13); H_\omega(11)$		673	677	669	$K_R(23); H_\beta(26)$
53	522		526	543	$H_\omega(22); H_\beta(33)$		514	515	527	$H_\omega(22); H_\beta(37)$
54	489		485	477	$H_\beta(28); H_\beta(16); H_\beta(10); H_\beta(33)$	458	454	458	$H_\beta(57); H_\beta(18); H_\beta(16)$	
55	450		452	456	$H_\beta(89)$	458	452	454	451	$H_\beta(54); H_\beta(16)$
56	401		398	410	$H_\beta(19); H_\beta(83); H_\beta(20)$	403	390	390	406	$H_\beta(19); H_\beta(59); H_\beta(16)$
57	328		322	329	$H_\beta(24); H_\beta(87)$	315	308	310	316	$H_\beta(11); H_\beta(33); H_\beta(60); H_\beta(15); H_\beta(14)$
58	299		288	292	$H_\beta(12); H_\beta(24); H_\beta(27)$	281	264	275	273	$H_\beta(10); H_\beta(60)$
59	235			238	$H_\beta(\text{Me})(97)$	175			170	$H_\beta(\text{Me})(97)$
60	116		122	120	$H_\beta(14); H_\beta(10); H_\beta(24); H_\beta(20)$	112		112	113	$H_\beta(14); H_\beta(11); H_\beta(23); H_\beta(20)$

^aThe average error is 5.44 cm⁻¹ or 0.62%.

influence of the Debye-Waller factor $\exp(-2W_d)$ may be neglected when comparing experimental and calculated spectra.¹⁸⁻²⁰

If one takes into account our experimental conditions, the intensity of the combination of a fundamental (S_f) with the lattice modes (S_L) can be approximated by

$$S_{\text{comb}} \propto S_f S_L / 2$$

In practice, the frequency distribution due to the lattice modes was fitted with a fourth-degree polynomial. Since the temperature of the samples was very low, only the positive combinations on the high-frequency side of the fundamentals were considered.

The application of this calculation for the three spectra investigated on the IN4 are shown in Figures 1c, 2c, and 3c. The calculated spectra which are shown in Figure 3b, and c, are based on the relative intensities of each deuterated compound in the mixture. It is evident that a perfect agreement between the experimental and calculated line shapes is unattainable in view

of the approximations involved in the calculations. One would also have to take into account the first overtone of the band centered around 240 cm⁻¹, which will be shown below to correspond to the methyl torsion, and which contributes to the intensity around 480 cm⁻¹. However, it can be seen that the agreement with the experimental data is better than when considering only the intensity due to the fundamentals (Figures 1b-3b).

Methyl Group Torsional Motion

The methyl group torsions are assigned from the NIS spectra since the intensity of these modes is very weak in optical spectroscopy. The methyl group torsional modes are expected to be intense in NIS because they involve large displacements of the hydrogen atoms. They are assigned at 240 (2a) and 235 cm⁻¹ (3a) for the hydrogenated compounds (the frequency difference is not significant due to the precision of the technique). These values fall in the range of the torsional frequencies observed for propane, isobutane, or neopentane.²¹⁻²³ These modes are not

(18) Jobic, H.; Ghosh, R. E.; Renouprez, A. *J. Chem. Phys.* **1981**, *75*, 4025.

(19) Griffin, A.; Jobic, H. *J. Chem. Phys.* **1982**, *75*, 5940.

(20) Warner, M.; Lovesey, S. N.; Smith, J. Z. *Phys. B.* **1983**, *51*, 109.

(21) Weiss, S.; Leroi, G. E. *Spectrochim. Acta, Part A* **1969**, *25*, 1759.

(22) Grant, D. M.; Pugmire, R. J.; Livingston, R. C.; Strong, K. A.; McMurry, H. L.; Brugger, R. M. *J. Chem. Phys.* **1970**, *52*, 4424.

TABLE III: Valence Force Constants for the 2-Methylnorbornanes^a

force constant	initial value	final value for 2	
		exo	endo
K_r	4.699	4.694	4.694
K_d	4.631	4.638	4.632
K_s	4.576	4.597	4.597
K_R	4.233	4.278	4.205
$K_{R'}$	4.521	4.544	4.869
$K_{R(Me)}$	4.387	4.493	4.324
H_α	0.540	0.540	0.556
H_β	0.645	0.655	0.653
H_δ	0.582	0.583	0.554
H_γ	0.610	0.595	0.639
H_ζ	0.559	0.472	0.617
$H_{\zeta'}$	0.657	0.583	0.758
H_ω	0.678	1.085	0.478
$H_{\omega'}$	0.618	0.587	0.578
H_ϕ	1.874	1.608	1.778
$H_{\phi'}$	1.460	1.798	1.529
$H_{\phi''}$	1.084	1.076	1.024
$H_{\phi'''}$	1.084	0.982	1.202
H_τ	0.055	0.000	0.153
$H_{\tau'}$	0.102	0.241	0.128
$H_{\tau''}$	0.062	0.166	0.107
$H_{\tau'''}$	0.070	0.047	0.048
$H_{\tau(Me)}$	0.120	0.117	0.112
F_d	-0.034	-0.029	-0.037
F_r	0.043	0.030	0.021
F_R	0.035	0.059	0.194
$F_{R-\gamma}$	0.258	0.181	0.210
$F_{R\omega}$	0.437	0.446	0.619
$F_{R-\gamma'}$	0.097	-0.014	0.028
F_β	-0.012	-0.036	-0.025
F_γ	-0.071	-0.047	-0.047
F_ϕ	0.281	0.342	0.238
$F_{\phi''\phi'''}$	-0.041	-0.129	0.231
$F_{\gamma'}$	-0.008	-0.045	0.023
$F_{\gamma\omega}$	-0.070	-0.061	-0.049
$f_{\phi''\phi'''}$		0.137	0.527
$f_{\beta 0}$	-0.047	-0.005	-0.051
$f_{\gamma 0}$	0.009	-0.001	0.006
$f_{\gamma 180}$	-0.019	0.068	-0.007
$f_{\gamma 90}$	0.106	-0.008	0.128
$f_{\gamma\omega}$	-0.047	-0.058	0.047

^aNotations and units are taken from ref 16. The internal coordinates of the methyl group are defined in Figure 6.

observed in the corresponding optical spectra.

The methyl torsions are, however, not as prominent as can be expected. For compound **3a** the peak at 235 cm⁻¹ is the most intense (Figure 2a) but the calculated intensity is much larger. Thus the spectrum calculated with a fixed resolution and without the combinations with the lattice modes (Figure 2b) shows an intense peak at 235 cm⁻¹. For compound **2a**, the torsion at 240 cm⁻¹ is not the most intense experimental peak (Figure 1a) and the calculated spectrum, in figure 1b, reflects this discrepancy.

This surprising result has already been noticed for Mn(CO)₅CH₃,²⁴ but for the majority of previous calculations^{22,25,26} the agreement of the intensities was excellent. One possibility would be a mixing of the torsion with the other modes but the shift on deuteration $\nu_H/\nu_D = 1.35 \pm 0.02$ suggests that the methyl torsions are relatively pure motions (see also the PED in Tables I and II). The CD₃ torsions are indeed observed at 175 cm⁻¹ in Figure 3a; the low intensity of this band is due to the lower cross section of deuterium. The agreement with the experimental spectra is much better on introducing the instrumental resolution and the combination with the lattice modes, nevertheless a small difference remains. The only explanation is a broadening of the torsion peaks

which explains their relative low intensities. The width of these modes is indeed larger than the instrumental resolution, this effect being more important for the exo compound. We suggest that the shape of torsional potential is modified by intra- or intermolecular interactions. However, the only term that we can compute from the fundamental transition is the barrier height V_3 . Supplementary data would be necessary to obtain the value of V_6 .

Since the torsional frequencies for the 2-methylnorbornanes **2a** and **3a** are centered around 237 cm⁻¹, a threefold barrier height of 15.2 kJ mol⁻¹ can be calculated.^{27,28} This value is comparable to the barriers obtained for other simple hydrocarbons²¹ in the solid state.^{22,27}

Discussion of the Results

Evolution of the Force Constants. The final force field which is shown in Table III results from the best fit with the experimental frequencies (this force field is of course not unique). When compared to the initial force constants, the variations are small except for H_ω , H_ϕ , $H_{\phi'}$, and $F_{\phi''\phi'''}$ (and $f_{\phi''\phi'''}$) which correspond to valence angles. The variations of these force constants reflect the strain induced by the methyl group. These variations are significant but may be too large owing to the approximation used by the calculation of the G matrix: we have introduced the norbornane geometry, neglecting the bicyclic skeletal deformations induced by the methyl substituent (it has been shown that torsional angles deformations could be important⁴). A remark can be made for the $f_{\phi''\phi'''}$ force constants which correspond to an interaction between the angles C₆C₁C₂ and C₁C₂C₈ (see Figure 6). For aliphatic compounds these force constants depend on the dihedral angle of the four carbons but always are small.¹⁶ For the 2-methylnorbornanes **2** and **3**, the refinement gives respectively 0.137 and 0.557 mdyne Å rad⁻². The large difference between these two values reflects a specific interaction which depends on the position of the methyl group.

The calculated frequencies are listed in Tables I and II except for the 14 ν_{CH} which have been omitted. The overall average error between the experimental and calculated frequencies is of 0.61% or 5.2 cm⁻¹.

Description of the Low Frequencies (80–500 cm⁻¹). (1)-2-*exo*-Methylnorbornane (**2**). In the Raman spectrum, the three highest frequencies are polarized and the 471-cm⁻¹ line shows a low intensity. This mode corresponds to an antisymmetrical deformation of the skeleton with elongation/contraction along C₂C₅/C₃C₆, respectively (this mode is at 542 cm⁻¹ (A₂) for **1**). The mode at 437 cm⁻¹ is both a bridgehead deformation and a rocking motion of the 1-bridge CH₂ group (cf. 450 cm⁻¹ (B₂) for **1**). At 402 cm⁻¹ we find the "butterfly" or symmetrical vibration (cf. 410 cm⁻¹ (A₁) for **1**). The vibrations observed at 301 and 274 cm⁻¹ describe the skeletal twist (cf. 340 cm⁻¹ (B₁) for **1**) combined with the methyl group motion (CCC angle deformation) in two perpendicular directions. The pure methyl torsion was assigned at 240 cm⁻¹ while the 137-cm⁻¹ vibration corresponds to the antisymmetric torsion of the bicyclic skeleton (cf. 172 cm⁻¹ (A₂) for **1**). A remark can be made for the frequency at 137 cm⁻¹. In the corresponding vibration of norbornane, the C₇ methylene group is motionless along the symmetry axis while the C₂, C₃, C₅, and C₆ methylene groups move in an alternate manner. For **2a** the C₇ methylene group moves in opposite phase with the methyl group. This observation indicates for this mode either a mass effect or a through-space interaction between the two groups of atoms.

(2) 2-*endo*-Methylnorbornane (**3**). In the Raman spectrum of the endo derivative, the three highest frequency bands are also polarized but the 452-cm⁻¹ line shows the lowest intensity. Its corresponding normal coordinates describe the same atomic motion as for the exo compound. The mode at 485 cm⁻¹ describes the antisymmetrical deformation motion of the bicyclic skeleton, while

(23) Jobic, H.; Sportouch, S.; Renouprez, A. *J. Mol. Spectrosc.* **1983**, *99*, 47.

(24) Andrews, M. A.; Eckert, J.; Goldstone, J. A.; Passell, L.; Swanson, B. *J. Am. Chem. Soc.* **1983**, *105*, 2262.

(25) Brier, P. N.; Higgins, J. S.; Bradley, R. H. *Mol. Phys.* **1971**, *21*, 721.

(26) Rey-Lafon, M.; Filhol, A.; Jobic, H. *J. Phys. Chem. Solids* **1983**, *44*, 81.

(27) Durig, J. R.; Craven, S. M.; Harris, W. C. In "Vibrational Spectra and Structure", Durig, J. R., Ed; Dekker: New York, 1972; Vol. 1, p 73.

(28) Herschbach, D. R.; "Tables of Internal Rotation Problems", Harvard University, 1957.

TABLE IV: Thermodynamical Data of the 2-Methylnorbornanes 2a and 3a^a

	2a	3a
$S^\circ_T(\text{tr})$	180.958	180.958
$S^\circ_T(\text{r})$	114.893	114.600
$S^\circ_T(\text{v})$	163.511	162.507
$S^\circ_T(\text{m})$	5.774	5.774
S°_T	465.136	463.839
(c) TS°_T	266.523	265.779
(b) H°_T	76.860	76.525
(a) $1/2 \sum \hbar \omega$	520.699	521.452
$E = (a) + (b) - (c)$	331.036	332.198
ΔE		1.162
$\Delta G^\circ_T(\text{expt})$		3.720
$\Delta E_{\text{BO}}(\text{expt})$		2.558
$E_{\text{BO}}(\text{calcd})$	-179175.847	-179173.265
$\Delta E_{\text{BO}}(\text{calcd})$		2.582

^aThe entropy is in J K⁻¹ mol⁻¹; the energy is kJ mol⁻¹; $E_{\text{BO}}^{\text{calcd}}$ is calculated with the PCILO Method;^{29,2} tr = translation; r = rotation; v = vibration; m = mixing.

the mode at 452 cm⁻¹ is assigned to the bridgehead deformation and to the rocking of the 1-bridge CH₂ group. The "butterfly" motion is found at 398 cm⁻¹ while the skeleton deformations combined with the two motions of the methyl group are observed at 298 and 326 cm⁻¹. The torsional vibration of the methyl group was assigned at 235 cm⁻¹ and the antisymmetrical torsion of the bicyclic skeleton at 122 cm⁻¹. This skeletal vibration shows a large increase in the C₆ methylene motion, in opposite phase with the methyl group deformation. As for the exo compound these vibrations indicate a through-space interaction. We obtain the same information from the 298-cm⁻¹ vibrational mode, i.e., the methyl group moves in opposite direction to the nearest C₅ methylene group.

The difference for ν_{58} (12 cm⁻¹) and for ν_{60} (-17 cm⁻¹) between the endo and exo compounds depend on the relative interaction distances between the methyl group and the norbornane skeleton: $d(\text{C}_{\text{Me,endo}}-\text{C}_6) > d(\text{C}_{\text{Me,exo}}-\text{C}_7) > d(\text{C}_{\text{Me,endo}}-\text{C}_5)$. We shall give a quantitative interpretation of these results in a separate paper by treating the mono- and dimethyl derivatives together.

Calculation of Thermodynamic Values

In the vapor phase, the standard enthalpy H°_T and standard free enthalpy G°_T can be written

$$H^\circ_T = E_{\text{BO}} + \frac{1}{2} \sum_{k=1}^{3N-6} \hbar \omega_k + H^\circ_T(\text{ther})$$

$$G^\circ_T = H^\circ_T - TS^\circ_T$$

where E_{BO} is the fixed nucleus molecular energy of the molecule in the Born-Oppenheimer approximation (with an arbitrary energy zero), $1/2 \sum_{k=1}^{3N-6} \hbar \omega_k$ is the zero-point vibrational energy (ZPVE), and $H^\circ_T(\text{ther})$ is the thermal contribution to the enthalpy at the temperature T . TS°_T is the entropy term: when the translations, rotations, and vibrations are independent, the total entropy S°_T is the sum of the translation entropy $S^\circ_T(\text{tr})$, the rotation entropy $S^\circ_T(\text{r})$, the vibration entropy $S^\circ_T(\text{v})$ and, if subspecies are to be considered, the mixing entropy $S^\circ_T(\text{m})$.

In a previous paper² we have calculated these terms for various aliphatic, cyclic, and bicyclic compounds using the frequencies

obtained from molecular mechanics. The frequency values derived from molecular mechanics gave only the right order of magnitude for the free enthalpy difference ΔG°_T (there was a difference of 20% with the experimental value³). In this work we have performed the same calculations using the experimental frequencies and keeping the nonvibrational entropic terms unchanged.² The results are given in Table IV. In this table, E , which is defined as the sum of three terms, is not a standard notation; however, the free enthalpy difference between isomers can be written as $\Delta G^\circ_T = \Delta E + \Delta E_{\text{BO}}$. The experimental measurements of the standard free energy difference ΔG°_T through chemical equilibration of isomers 2a and 3a and the determination of the thermodynamic contributions ΔE lead to an experimental ΔE_{BO} value. The difference between the thermodynamic terms ΔE is 1.162 kJ mol⁻¹, that is 31% of the experimental ΔG°_T which is 3.274 kJ mol⁻¹.³ It represents a large contribution which can never be omitted in energetic comparisons of isomers by ab initio methods as well as in molecular mechanics. The experimental ΔE_{BO} value which is deduced is 2.558 kJ mol⁻¹; the corresponding value obtained by the PCILO method²⁹ is 2.582 kJ mol⁻¹,² and thus the agreement is better than 1% (Table IV).

To emphasize the effect of the low frequencies it can be noted that the energy difference obtained from the seven lowest frequencies is 0.224 kJ mol⁻¹, that is, 19% of the total contribution and 6% of the standard free energy difference. (The difference between the lowest frequency of the two isomers is -0.557 kJ mol⁻¹.)

Conclusion

From a combination of the infrared, Raman, and NIS data for the 2-methylnorbornanes, we have satisfactorily assigned the low-frequency region; however, the assignment of several high-frequency modes is only tentative.

The simulation of the low-frequency NIS spectra was improved by considering, in addition to the fundamentals, combinations with the lattice mode. A comparison between the two isomers shows the important role of the vibrational modes to the free enthalpy difference.

This vibrational analysis has allowed us to differentiate the force constants of the methyl group in exo or endo position. The determination of the force field for the 2-methylnorbornanes was necessary for our next step which is a study of the dimethylnorbornanes 4-6.

Acknowledgment. We are very much indebted to A. Chosson and A. Corne (Laboratoire de Spectroscopie Optique, Université de Savoie, Chambéry, France) for their help in recording the Raman spectra. We thank Dr. J. C. Lassègues and Dr. B. Desbat (Laboratoire de Spectroscopie Infrarouge, Bordeaux, France) for their careful investigation of the infrared spectra, O. Martin-Borret for her participation in the synthesis, and S. Lavaitte for the modifications of program of simulated spectra.

Registry No. 2a, 872-78-6; 2b, 94427-75-5; 3a, 765-90-2; 3b, 94427-76-6; 7, 934-30-5; 8, 1195-12-6; 9, 769-85-7; 10, 2903-75-5; 11, 7732-50-5; 12, 13360-81-1; cyclopentadiene, 542-92-7; acrylic acid, 79-10-7; methyl acrylate, 96-33-3; neutron, 12586-31-1.

(29) Malrieu, J. P. in "Semiempirical Methods of Electronic Structure Calculation, Part A: Techniques", Segal, G. A., Ed.; Plenum Press: New York, 1977; p 90.